

## Impact of Alginate Conditioning Film on Deposition Kinetics of Motile and Nonmotile *Pseudomonas aeruginosa* Strains<sup>∇</sup>

Alexis J. de Kerchove and Menachem Elimelech\*

Department of Chemical Engineering, Environmental Engineering Program, Yale University,  
P.O. Box 208286, New Haven, Connecticut 06520-8286

Received 25 March 2007/Accepted 8 June 2007

**The initial deposition of bacteria in most aquatic systems is affected by the presence of a conditioning film adsorbed at the liquid-solid interface. Due to the inherent complexity of such films, their impact on bacterial deposition remains poorly defined. The aim of this study was to gain a better understanding of the effect of a conditioning film on the deposition of motile and nonmotile *Pseudomonas aeruginosa* cells in a radial stagnation point flow system. A well-defined alginate film was used as a model conditioning film because of its polysaccharide and polyelectrolyte nature. Deposition experiments under favorable (nonrepulsive) conditions demonstrated the importance of swimming motility for cell transport towards the substrate. The impact of the flagella of motile cells on deposition is dependent on the presence of the conditioning film. We showed that on a clean substrate surface, electrostatic repulsion governs bacterial deposition and the presence of flagella increases cell deposition. However, our results suggest that steric interactions between flagella and extended polyelectrolytes of the conditioning film hinder cell deposition. At a high ionic strength (100 mM), active swimming motility and changes in alginate film structure suppressed the steric barrier and allowed conditions favorable for deposition. We demonstrated that bacterial deposition is highly influenced by cell motility and the structure of the conditioning film, which are both dependent on ionic strength.**

Biofilm formation or biofouling, a widespread problem in aquatic environments, can negatively affect processes in natural, engineered, and biomedical systems, resulting in contaminated aquifers (25), fouled membranes (3), and infected catheters and biomedical implants (40). The accumulation of metabolically active microorganisms on surfaces can lead to material degradation and affect system performance through energy cost increases and reduction in expected life spans. Biofouling control remains a major challenge because of the intricate processes involved in biofilm development, such as bacterial deposition, growth, and maturation (10). A better understanding of bacterial deposition—the step that initiates biofouling—can be used to develop improved control and prevention strategies in order to reduce the adverse impacts of biofilms on aquatic environments.

Most fundamental studies have investigated the initial deposition of microbes in oversimplified systems using ultraclean surfaces as a surrogate for the solid-liquid interface (19, 21). However, the properties of the solid-liquid interface are altered by the adsorption of polyelectrolytes, such as humic substances and polysaccharides in natural aquatic systems (31) and glycoproteins, lipids, and nucleotides in biomedical systems (1). Because of its charged and macromolecular nature, this polyelectrolyte film, known as the conditioning film, changes the physicochemical properties of the surface (37) (e.g., surface roughness and surface charge distribution), which affects bacterial deposition (42). The conditioning film can also modify the biological properties of a substrate and induce

specific responses in the microorganism, such as chemotaxis and attachment to specific receptors (7).

Previous studies on the role of the conditioning film in bacterial adhesion and deposition have demonstrated the major influence of the film on bacterial adhesion (4, 43). Observations of the enhancement or inhibition of cell deposition were attributed to differences in the levels of surface hydrophobicity of the depositing strains. However, because of the inherent complexity of the conditioning films used, these studies were unable to provide a more complete mechanistic interpretation of the interactions involved in the deposition process. Therefore, a more gradual and systematic approach to increasing the complexity of the conditioning film is required to investigate the effects of adsorbed polyelectrolytes on substrate properties and subsequently on the deposition of microorganisms.

Ideally, the model macromolecular constituents of the film need to (i) be a well-characterized polymer that is representative of the properties of the conditioning film of interest, (ii) form well-defined layers by adsorption to the substrate, and (iii) significantly alter the physicochemical and biological properties of the substrate after adsorption. Alginate layers are likely to approach these features because of their nature, source, and characterization. The polysaccharide and polyelectrolyte nature of alginate makes it an excellent candidate to approximate the dissolved organic matter present in aquatic environments and wastewater effluents (26). Alginate is also an exogenic product of bacteria and is likely to stimulate a biological response in planktonic microorganisms (18). Alginate assemblies form homogeneous thin layers and exhibit dynamic viscoelastic properties in response to changes in the ionic composition of the surrounding solution (14). The alginate film is a well-defined structure with moderate complexity and can be

\* Corresponding author. Mailing address: Department of Chemical Engineering, Environmental Engineering Program, Yale University, P.O. Box 208286, New Haven, CT 06520-8286. Phone: (203) 432-2789. Fax: (203) 432-2881. E-mail: menachem.elimelech@yale.edu.

<sup>∇</sup> Published ahead of print on 15 June 2007.

TABLE 1. Strains, plasmids, and primers used for the construction of the PAO1  $\Delta fliC$   $\Delta pilA$ , PAO1  $\Delta fliC$ , and PAO1  $\Delta pilA$  strains

Strain, plasmid, or primer	Relevant characteristics	Source
<b>Strains</b>		
<i>E. coli</i>		
XL1-Blue	<i>recA1 endA1 gyrA96 thi-1 hsdR17 supE44 relA1 lac</i> [F' <i>proAB lacI<sup>q</sup>Z</i> $\Delta$ M15 Tn10 (Tc <sup>r</sup> )]	Stratagene
S17-1	Used for mating constructs into <i>P. aeruginosa</i> ; <i>thi pro hsdR recA</i> RP4-2 plasmid (Tc::Mu) (Km::Tn7)	Laboratory of Barbara Kazmierczak
<i>P. aeruginosa</i>		
PAO1	Wild-type <i>P. aeruginosa</i> strain ATCC 15692	
PAO1 $\Delta fliC$	PAO1 with in-frame deletion of <i>fliC</i> ; Tc <sup>r</sup>	This study
PAO1 $\Delta pilA$	PAO1 with in-frame deletion of <i>pilA</i>	
PAO1 $\Delta fliC$ $\Delta pilA$	PAO1 with in-frame deletion of <i>fliC</i> and <i>pilA</i> ; Tc <sup>r</sup>	This study
<b>Plasmids</b>		
pGEM-T Easy	<i>E. coli</i> TA cloning vector; Ap <sup>r</sup>	Promega
pEX18Gm	Allelic replacement suicide plasmid; Ap <sup>r</sup> (Cb <sup>r</sup> ) <i>sacB</i> oriT	
pEX18- $\Delta fliC$	Gene regions flanking <i>fliC</i> (corresponding to the N and C termini) and Tc <sup>r</sup> gene cloned in tandem into pEX18Gm; Ap <sup>r</sup> (Cb <sup>r</sup> ) Tc <sup>r</sup>	This study
pEX18Gm- $\Delta pilA$	Gene regions flanking <i>pilA</i> (corresponding to the N and C termini) and Tc <sup>r</sup> gene cloned in tandem into pEX18Gm; Ap <sup>r</sup> (Cb <sup>r</sup> ) Tc <sup>r</sup>	This study
<b>Primers<sup>a</sup></b>		
<i>fliC</i> -N1	CAA TTG GTG GAC TGG GTG TTC TTC G	This study
<i>fliC</i> -N2	GGA TCC GCG GCC GCG GTC AGA GCG TGC AAC GAG G	This study
<i>fliC</i> -C1	GGA TCC GCG GCC GCT GTC GAA GAA CCA GGT GC	This study
<i>fliC</i> -C2	AAG CTT GCA ATC TTG CTG CTG GTG GC	This study

<sup>a</sup> The sequences of all primers are listed 5' to 3'.

used as a preliminary surrogate for conditioning films formed in natural and engineered aquatic systems.

In contrast with the conditioning film, the bacterial surface is a relatively well-characterized assembly of dynamic appendages that enable the microbial transition from a planktonic to a sessile state (33, 46). Among these appendages, flagella are actively involved in the transport of the microorganism towards the substrate (8), as well as in the initial deposition (34) and occasional detachment of the microorganism (27). The rotation of the flagella, which enables cell transport, is driven by the coupling of electrochemical potentials across the cell membrane and electrostatic interactions between fixed charges on the flagella and the proton flux across the membrane (5). In the vicinity of the substrate, physicochemical and biological interactions between the substrate and the flagellins—glycosylated subunits of the filament (44)—can affect the deposition behavior of the cells (34). Because of these flagellar functions and the paramount importance of flagella in the settling of microorganisms, these appendages are often indicated to be the mediators of the virulence of pathogenic bacteria (22). A better understanding of the environmental factors affecting the flagellar functions would have tremendous impact on the prevention of infectious diseases. However, there is minimal research that addresses the effects of the presence of a well-defined conditioning film on the deposition behavior of motile bacteria.

In this work, we studied the kinetics of the deposition of motile and nonmotile bacteria onto conditioned surfaces under laminar flow to determine the role of cell motility and the role of the conditioning film in bacterial deposition. Experiments were conducted using an alginate layer as a model con-

ditioning film and *Pseudomonas aeruginosa* PAO1 as a model bacterial species. PAO1 is a well-characterized pathogen that is extremely active in the biofouling of substrates in natural and engineered aquatic systems (20). Genetically modified PAO1 was used to determine the impact of flagellar motility on cell deposition. We demonstrated that the kinetics of the deposition of motile bacteria onto alginate films exhibited a unique dependence on ionic strength, with a maximum deposition rate obtained when the electrolyte concentration of the solution approached physiological conditions.

#### MATERIALS AND METHODS

**Construction of the *P. aeruginosa* strains.** Bacterial strains listed in Table 1 were cultured in Luria-Bertani (LB) or Vogel-Bonner minimal (VBM) medium at 37°C. The conditions and procedures used for strain construction were similar to those detailed by Kazmierczak et al. (23) and are summarized below. Chromosomal and plasmid DNA, ligation reaction and PCR mixtures, and Southern blots were prepared according to standard protocols (2). The *fliC*::Tc<sup>r</sup> cassette was constructed using primers (Invitrogen) designed from the PAO1 genome sequence (<http://www.pseudomonas.com>) (39). The primer pairs *fliC*-N1/*fliC*-N2 and *fliC*-C1/*fliC*-C2 (Table 1) were used to amplify the gene regions flanking *fliC* and corresponding to the N and C termini of the gene product by using PAO1 genomic DNA as a template. The amplified regions were subcloned into the allelic exchange vector pEX18Gm (38). A tetracycline resistance cassette was subsequently subcloned between the flanking regions to make pEX18- $\Delta fliC$ . *Escherichia coli* S17-1 cells were transformed with this construct, which was then introduced into PAO1 through mating. Gentamicin-resistant exconjugants (merodiploids) were isolated on VBM medium plus gentamicin (100  $\mu$ g/ml) and then resolved by growth on VBM medium containing tetracycline (100  $\mu$ g/ml) plus 5% sucrose as described by Schweizer and Hoang (38). Mutants were screened by PCR and verified by Southern blotting (data not shown). The vector pEX18Gm- $\Delta pilA$ , which contains the regions flanking *pilA* and corresponding to the N and C termini of the gene product, was kindly provided by B. I. Kazmierczak (Yale University). This construct was introduced into PAO1 and the PAO1  $\Delta fliC$

strain, and the single- and double-knockout PAO1  $\Delta pilA$  and PAO1  $\Delta fliC \Delta pilA$  strains were selected as described above. The deletion of *pilA* was confirmed with Southern blotting (data not shown). In contrast to the wild type, the mutant PAO1  $\Delta fliC$  and PAO1  $\Delta fliC \Delta pilA$  strains did not spread on 0.3% agar-LB plates and did not exhibit any swimming motility when observed under a microscope. The mutant PAO1  $\Delta pilA$  and PAO1  $\Delta fliC \Delta pilA$  strains did not exhibit any twitching motility on 1.5% agar-LB plates.

**Cell preparation and characterization.** The following protocol was applied to all cell cultures used in the characterization or deposition kinetics experiments. PAO1 strains were incubated in LB at 37°C and harvested at mid-exponential growth phase. The bacterial suspension was centrifuged (in a Sorvall RC 26 Plus) for 15 min at 1,000  $\times g$ . The cell pellet was washed once with 100 mM KCl solution, recentrifuged under the same conditions, and finally resuspended in KCl (100 mM).

Transmission electron micrographs were obtained using a Tecnai 12 Biotwin microscope. Samples of planktonic and sessile cells were collected either from the liquid cultures or from the periphery of a solid colony growing on a 1.5% agar-LB plate. Samples were resuspended in deionized water and adsorbed to glow-discharged carbon grids for 1 min. Grids were stained for 2 min in 2% uranyl acetate, washed with deionized water twice for 20 s each, and then briefly dried before imaging.

Measurements of bacterial electrophoretic mobility were performed with a ZetaPALS analyzer (Brookhaven Instruments Corp., NY) according to procedures previously described by de Kerchove and Elimelech (13). Electrophoretic mobility measurements were converted into zeta potentials by using the Smoluchowski equation. This equation was applicable because of the relatively large cells and the ionic strengths used (17). The relative level of hydrophilicity of the cells of each PAO1 strain was measured using the microbial-adhesion-to-hydrocarbons test with *n*-dodecane (laboratory grade; Fisher Scientific) (32). Hydrophilicity is defined here as the fraction of total cells partitioned into the aqueous phase. The surface acidity of the cells of each strain was determined by titration using hexadimethrine bromide (Sigma, MO) and poly(vinyl sulfate) potassium salt (Sigma, MO) as cationic and anionic standards, respectively (24). The surface charge density was calculated using the average ellipsoid superficial area of the bacterial cells.

The average bacterial size was determined as a function of ionic strength by contrast-phase microscopy. More than 100 discrete bacterial cells for each ionic condition were studied. The average major and minor axes were calculated with MATLAB software (The MathWorks Inc., MA) by assuming an ellipse with the same second moments as those for rod-shaped bacteria. Cell viability tests were performed with a BacLight viability kit (Molecular Probes, OR), which uses fluorescence to detect stained dead and live cells. Cell viability was studied as a function of ionic strength.

**Substrate preparation and characterization.** Ultrapure quartz coverslips measuring 25 mm in diameter and 0.1 mm thick (Electron Microscopy Sciences, PA) were used in the deposition experiments. Quartz slips were cleaned using a three-step procedure. Organics were removed by soaking the coverslips overnight in 2% Hellmanex II solution (Hellma GmbH and CoKG, Germany) at 75°C and then rinsing them with deionized water. To remove metal impurities, the quartz slips were soaked overnight in Nochromix solution (Godax Laboratories, Inc., MD) at room temperature and rinsed with deionized water. Finally, the residual carbon impurities were removed by baking the coverslips at 560°C for 1 to 3 h.

Conditions favorable (nonrepulsive) for the deposition of the cells onto the substrate were obtained by the chemical modification of the coverslip surface. Charge reversal was induced by the adsorption of a layer of poly-L-lysine (PLL) at the quartz surface. PLL hydrobromide (Sigma, MO) has an average molecular mass of 110 kDa. The quartz coverslips were submerged in a 0.1-g/liter solution of 0.22- $\mu$ m-pore-size-filtered PLL-HEPES (pH 5.6) overnight at 4°C and rinsed four times with 0.22- $\mu$ m-pore-size-filtered deionized water. The quartz coverslips were dried for 3 h in a vacuum at 37°C. Bacterial deposition experiments were performed under favorable conditions over a wide range of ionic strengths (1 to 100 mM) and at an ambient pH (5.4 to 5.6).

Alginate conditioning films were formed by the adsorption of dispersed alginate (0.1 g/liter in a 10 mM KCl solution) for 15 min onto PLL-coated quartz under laminar flow conditions. We used commercial sodium alginate (Sigma, MO) with an average molecular mass of 72.7 kDa. The alginate films were rinsed for 15 min with the electrolyte solution of interest prior to the bacterial deposition experiment in a radial stagnation point flow (RSPF) system (14).

To characterize the electrokinetic properties of the clean and coated quartz, 1.6- $\mu$ m-diameter silica particles (Bangs Laboratories, Inc., IN) were used as a surrogate for the quartz slides. Conditioned silica particles were obtained by successively dispersing the particles in PLL and alginate solutions. Particles were

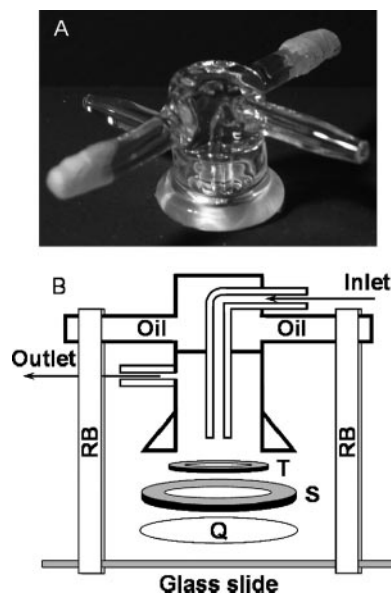


FIG. 1. Specially designed RSPF system for studying bacterial deposition kinetics in real time: picture (A) and diagram (not to scale) (B). “Oil” shows the location of the mineral oil chamber. Q is for quartz coverslip, RB is for rubber band, S is for silicon sealing strip, and T is for Teflon spacer.

extracted from overnight suspensions by centrifugation (1,000  $\times g$  for 1 min). The electrophoretic mobility measurements and the sizes of the clean and coated particles as a function of ionic (KCl) strength were determined using ZetaPALS (Brookhaven Instruments Corp., NY). Electrophoretic mobility measurements were converted into zeta potentials by using the Smoluchowski equation.

**RSPF system.** Bacterial deposition rates were studied in a well-controlled RSPF system. Deposited bacterial cells were observed in a novel, specially designed glass flow chamber (Fig. 1A) mounted onto the stage of an inverted microscope (Axiovert 200m; Zeiss) operating in the contrast phase. A separate chamber filled with mineral immersion oil (type DF; Cargille Laboratories Inc., NJ) was mounted onto the RSPF flow cell to minimize the transitions in the refraction index (refraction index of the oil  $\approx$  refraction index of the glass  $\approx$  1.52) and the scattering of the light between the light source and the collector surface. Bacterial cell deposition was recorded at regular intervals (10 to 20 s) for 10 min with a DP70 digital camera (Olympus). The quartz collector surface was sealed to the open bottom side of the glass chamber with a silicon sealing strip (Dow Corning, CA) and maintained at a constant distance from the capillary with a Teflon spacer (Fig. 1B). The sealing system was compressed by clamping the glass chamber to a larger glass slide. The hydrodynamics of the system have been well defined previously (11) and were confirmed for the specific dimensions of our flow cell (FEMLAB; COMSOL). The injection capillary has a diameter of 2 mm, with a 2-mm distance between the outlet of the capillary and the collector surface. During experiments, a constant flow of 4.93 ml/min (capillary average velocity, 2.65 cm/s) was induced by syringe pumps (KD Scientific Inc., New Hope, PA). The Reynolds number at the outlet of the capillary was 28.4, resulting in a bacterial cell Peclet number of 0.22 (17). All results were obtained under the same hydrodynamic conditions and at 25°C ( $\pm 1^\circ$ C).

**Deposition kinetics protocol.** Bacterial cell deposition as a function of ionic strength in monovalent (KCl) salt at an ambient (unadjusted) pH (5.4 to 5.6) was studied. Electrolyte solutions were prepared with deionized water and reagent-grade salt (Fisher Scientific) and stored at 4°C. For each cell culture, the cell concentration was determined in a Bürker-Türk cytometer chamber (Marienfeld Laboratory Glassware, Germany). Prior to each experiment, concentrated cell suspensions were diluted with the electrolyte solution of interest.

From a single bacterial deposition experiment, the bacterial transfer rate coefficient was calculated as the ratio between the bacterial deposition flux and the initial bacterial bulk concentration (46). The bacterial deposition flux was the observed deposition rate of bacteria as normalized by the camera viewing area. Bacterial deposition kinetics were represented as the attachment (or deposition) efficiency (16). The attachment efficiency corresponded to the bacterial transfer

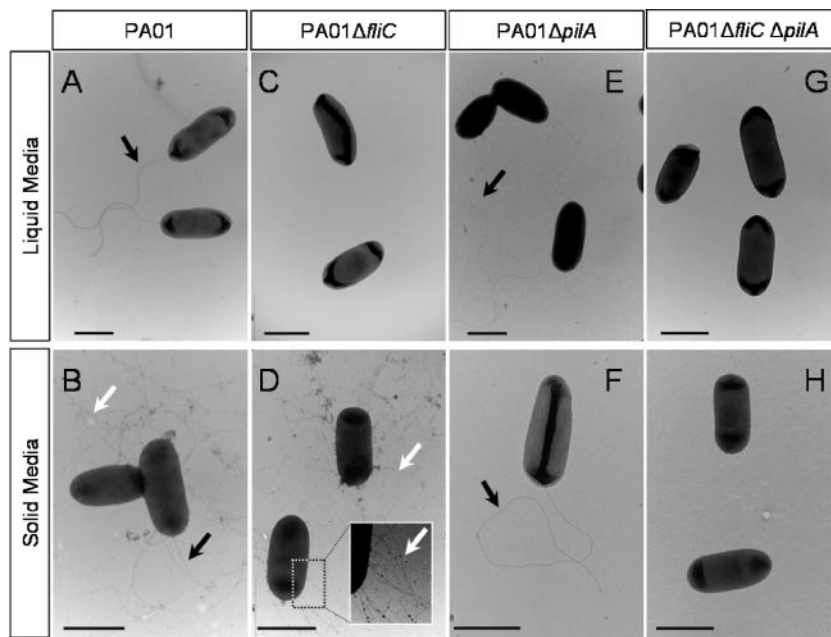


FIG. 2. Transmission electron micrographs of representative cells characterizing the four genetically modified PAO1 strains. Cells from cultures on liquid and solid media are shown. The scale bars represent 1  $\mu\text{m}$ . Black arrows show flagella, and white arrows show pili.

rate coefficient normalized by the bacterial transfer rate coefficient measured under favorable (nonrepulsive) conditions. Reported attachment efficiency values are averages of data taken from two to four experiments conducted using discrete cell cultures.

## RESULTS AND DISCUSSION

**Characteristics of genetically modified PAO1 strains.** Three genetically modified *P. aeruginosa* PAO1 strains, constructed by allelic displacement, were used: (i) the PAO1  $\Delta$ *fliC* strain, deficient in the biosynthesis of flagellar proteins; (ii) the PAO1  $\Delta$ *pilA* mutant, deficient in the biosynthesis of type IV pilus proteins; and (iii) the PAO1  $\Delta$ *fliC*  $\Delta$ *pilA* strain, deficient in the biosynthesis of both flagellar and type IV pilus proteins. We determined the morphological and physiological properties of the cells, as well as cell surface physicochemical properties, for the three mutant strains and the wild-type PAO1.

The morphological features of planktonic and sessile cells were studied by transmission electron microscopy (Fig. 2). Flagella were present at the surfaces of planktonic and sessile cells of PAO1 and the PAO1  $\Delta$ *pilA* mutant. Type IV pili were produced only on the surfaces of sessile cells of PAO1 and the PAO1  $\Delta$ *fliC* strain. The primary function of type IV pili is to enable the twitching motility of sessile cells (29), and therefore, the presence of pili at the surfaces of planktonic cells was not anticipated. The absence of flagella at the surfaces of PAO1  $\Delta$ *fliC* and PAO1  $\Delta$ *fliC*  $\Delta$ *pilA* cells and the absence of type IV pili at the surfaces of PAO1  $\Delta$ *pilA* and PAO1  $\Delta$ *fliC*  $\Delta$ *pilA* cells confirm the swimming and twitching disabilities of the strains, respectively.

Because deposition kinetics are sensitive to the sizes and physiological states of cells (45), we characterized the variation in size and viability of PAO1  $\Delta$ *pilA* and PAO1  $\Delta$ *fliC*  $\Delta$ *pilA* cells as a function of ionic (KCl) strength. These two mutant strains were selected to ensure the absence of type IV pili at the

surfaces of planktonic cells in order to study the impact of swimming motility on deposition. Both PAO1  $\Delta$ *pilA* and PAO1  $\Delta$ *fliC*  $\Delta$ *pilA* cells had major and minor axes of  $2.25 \pm 0.15$  and  $0.93 \pm 0.01$   $\mu\text{m}$ , respectively, which is equivalent to a volumetric spherical diameter of 1.24  $\mu\text{m}$ . No significant differences in size over a range of ionic strengths (1 to 1,000 mM KCl) were observed. Viability tests over the same range of ionic strengths demonstrated that PAO1  $\Delta$ *pilA* and PAO1  $\Delta$ *fliC*  $\Delta$ *pilA* cells were sensitive to low ionic strength, maintaining a viability of 59% ( $\pm 11\%$ ) at ionic strengths below 10 mM. However, the viability of the cells quickly increased to a stable value of 81% ( $\pm 8\%$ ) at ionic strengths above 10 mM. High osmotic pressure and electrolyte imbalance across the cell membrane are likely to be the causes of the high lethality observed at low ionic strengths (35).

The presence of the flagella is likely to change the surface properties of the bacteria. Hydrophilicity tests and titration to determine surface acidity demonstrated statistically significant differences between motile (PAO1 and PAO1  $\Delta$ *pilA*) and nonmotile (PAO1  $\Delta$ *fliC* and PAO1  $\Delta$ *fliC*  $\Delta$ *pilA*) strains (Fig. 3). Motile strains had an average cell surface acidity of  $(10.6 \pm 0.5) \times 10^{-6}$  meq/ $10^8$  cells, compared to  $(7.0 \pm 1.0) \times 10^{-6}$  meq/ $10^8$  cells for nonmotile strains, and an average hydrophilicity of  $93\% \pm 1\%$ , compared to  $82\% \pm 2\%$  for the nonmotile strains. These values are comparable to previously published data on PAO1 (41, 45).

Measurements of the cell surface acidity can be converted into surface charge densities by assuming a homogeneous distribution of acidic functional groups over the surface area of the cell. Because of the similarity in size between the cells of the PAO1 wild-type and mutant strains, we calculated an average ellipsoid surface area of the cell bodies of 1.71  $\mu\text{m}^2$ . For the two motile strains, an additional 0.57  $\mu\text{m}^2$  was added to this calculated body surface area to account for the flagella, cylin-

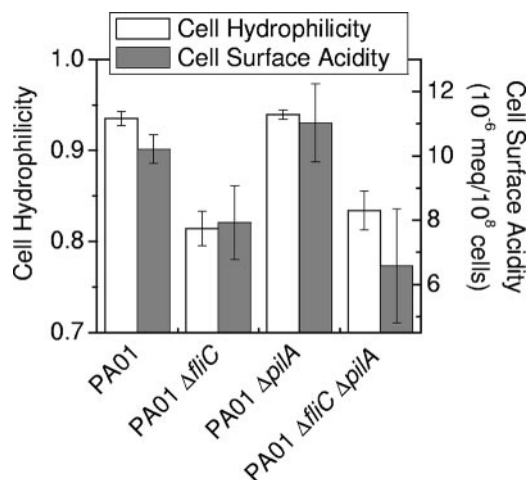


FIG. 3. Estimates of the cell hydrophilicity and surface acidity levels of each PAO1 strain. Hydrophilicity was measured using the microbial-adhesion-to-hydrocarbons test (32) and is represented as the fraction of cells partitioned into the aqueous phase. The surface acidity of the cells was determined by titration using hexadimethrine bromide and polyvinyl sulfate as cationic and anionic standards, respectively (24).

drical structures measuring 18 nm in diameter and 10  $\mu$ m in length (12), to obtain a total surface area of 2.28  $\mu$ m<sup>2</sup>. Applying these two surface areas, we calculated a statistically equivalent surface charge density of  $430 \pm 40 \mu$ C/cm<sup>2</sup> for the four PAO1 strains. This result suggests that the greater acidity of the motile cells and their enhanced affinity for the aqueous phase, as discussed above, result from the presence of the flagella at the bacterial surface. Three aspects of the flagellar structure and function are likely to affect the cell surface properties: (i) the glycosylation of flagellins that are present in up to 20,000 copies (44), (ii) the presence of charged residues ubiquitous in the protein structures that form the basal bodies, the hooks, and the filaments of the flagella (47), and (iii) the transmembrane ion currents that drive the rotation of the basal bodies (5).

**Electrophoretic mobility measurements and zeta potentials of cells and the substrate.** Electrophoretic mobility measurements for the motile PAO1  $\Delta$ pilA and nonmotile PAO1  $\Delta$ fliC  $\Delta$ pilA strains give an estimate of the zeta potentials at the surfaces of the cells (Fig. 4). The two strains had comparable zeta potentials over the studied range of ionic strengths. The negative zeta potentials decreased in magnitude as the ionic strength of the solution increased and approached a nonzero, residual value at high ionic strengths. This behavior is characteristic of “soft” particles coated with a polyelectrolyte layer, such as bacterial cells with charged exopolymeric substances at their surfaces (13). The equivalence of the zeta potentials of the two strains strongly corresponds to the similarities in calculated surface charge density among the strains.

Electrophoretic mobility measurements of 1.6- $\mu$ m-diameter SiO<sub>2</sub> particles were used to estimate the zeta potentials of clean and coated quartz substrates (Fig. 5). Clean particles were highly negatively charged and had negative zeta potentials that approached zero at high ionic strengths. The PLL coating of the SiO<sub>2</sub> particles induced charge reversal, as dem-

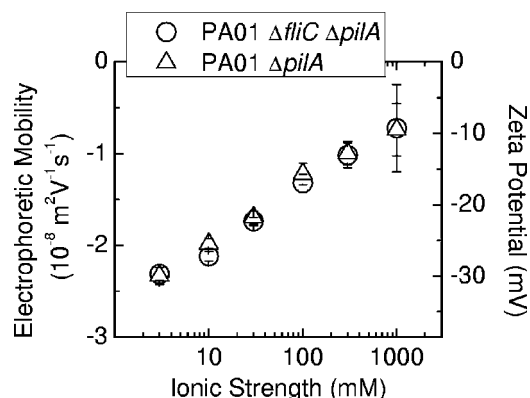


FIG. 4. Electrophoretic mobility measurements and calculated zeta potentials of PAO1  $\Delta$ fliC  $\Delta$ pilA and PAO1  $\Delta$ pilA cells as a function of ionic (KCl) strength. Measurements were carried out at an ambient (unadjusted) pH (5.4 to 5.6) and a temperature of 25°C ( $\pm$ 1°C). Error bars indicate 1 standard deviation.

onstrated by positive zeta potentials. The subsequent adsorption of negatively charged alginates at the surfaces of PLL-coated particles induced a second reversal of the surface charge, as suggested by negative zeta potentials. In contrast with the clean SiO<sub>2</sub> particles, the coated particles had nonzero zeta potentials at high ionic strengths, which confirms the presence of a soft polyelectrolyte layer at their surfaces (13). The diameters of SiO<sub>2</sub> particles in deionized water were  $1.57 \pm 0.05$

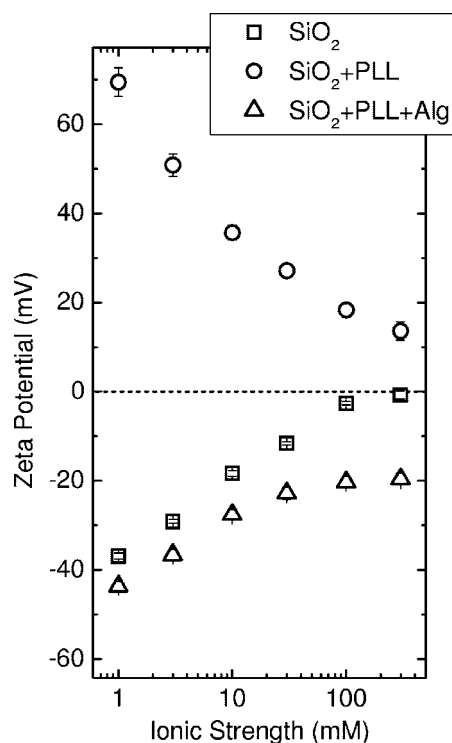


FIG. 5. Calculated zeta potentials of bare and film-coated silica particles as a function of ionic (KCl) strength. Measurements were carried out at an ambient (unadjusted) pH (5.4 to 5.6) and a temperature of 25°C ( $\pm$ 1°C). Error bars indicate 1 standard error. Alg, alginate.

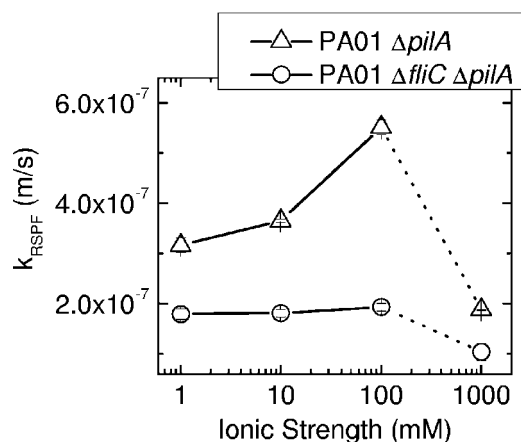


FIG. 6. Deposition kinetics of PAO1  $\Delta pilA$  and PAO1  $\Delta fliC \Delta pilA$  strains under favorable (nonrepulsive) conditions as a function of ionic (KCl) strength. The deposition kinetics are expressed as the cell transfer rate coefficient,  $k_{RSPF}$ . The capillary flow rate in the RSPF system was fixed at 4.93 ml/min (average velocity of 26.5 cm/s), resulting in a capillary Reynolds number of 28.4 and a particle (cell) Peclet number of 0.22. Other experimental conditions employed were an ambient (unadjusted) pH (5.5 to 5.7) and a temperature of 25°C ( $\pm 1^\circ$ C). Error bars indicate 1 standard deviation.

$\mu\text{m}$ ,  $2.08 \pm 0.17 \mu\text{m}$ , and  $1.95 \pm 0.11 \mu\text{m}$  for clean, PLL-coated, and alginate-PLL-coated particles, respectively. Therefore, minimal aggregation among the particles during the adsorption of polyelectrolytes was observed.

**Bacterial deposition kinetics under favorable (nonrepulsive) conditions.** Rate coefficients for the deposition of motile PAO1  $\Delta pilA$  and nonmotile PAO1  $\Delta fliC \Delta pilA$  cells onto PLL-coated quartz were determined as a function of ionic (KCl) strength (Fig. 6). Deposition kinetics under favorable (nonrepulsive) conditions were indicative of the convective-diffusion limit of microbial transport towards the substrate. Cell transfer coefficients for nonmotile bacteria remained constant at  $(1.84 \pm 0.07) \times 10^{-7}$  m/s with increasing ionic strength (1 to 100 mM). Cell transfer coefficients for motile bacteria under favorable conditions were at least two times higher than those for the nonmotile strains and significantly increased with increasing ionic strength, approaching a maximum of  $(5.51 \pm 0.15) \times 10^{-7}$  m/s at 100 mM. However, deposition rates for both bacterial strains dropped significantly at an ionic strength of 1,000 mM.

High deposition rates observed for motile bacteria are attributable to the ability of the cells to swim towards the surface. However, the sudden increase in the cell transfer rate observed at 100 mM was not anticipated. This deposition behavior contradicts the classical electrostatic-double-layer theory, which suggests that an increase in ionic strength reduces the range of attractive interactions and subsequently decreases or maintains the deposition rate of particles (15), as observed for nonmotile bacteria. The enhanced deposition rate of motile bacteria at 100 mM suggests that flagellar functions are strongly dependent on ionic strength. The reduction in the transfer rate at an ionic strength of 1,000 mM may be attributed to (i) the desorption of PLL from the quartz surface, which would create charge heterogeneity at the substrate surface and reduce attractive interactions, and (ii) the increase in the viscosity of the

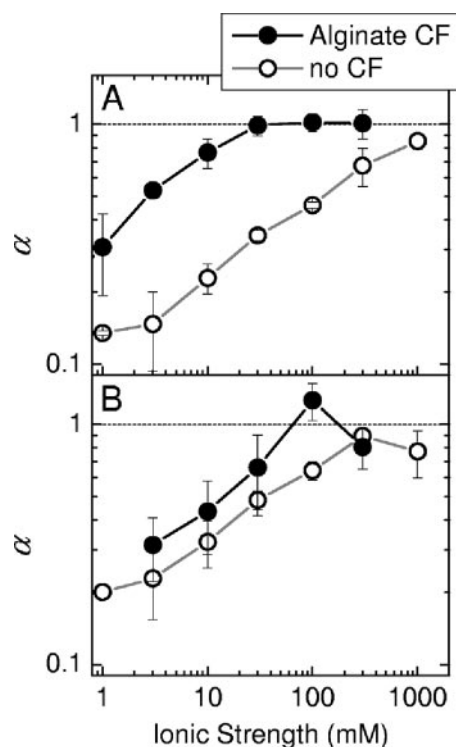


FIG. 7. Kinetics of the deposition of PAO1  $\Delta fliC \Delta pilA$  cells (A) and PAO1  $\Delta pilA$  cells (B) onto a clean quartz surface (no conditioning film [no CF]) and an alginate-coated quartz surface (alginate CF) as a function of ionic (KCl) strength. The deposition kinetics are expressed as the attachment (deposition) efficiency,  $\alpha$ , relative to the maximum efficiency, which was set at 1 (dotted lines). The capillary flow rate in the RSPF system was fixed at 4.93 ml/min (average velocity of 26.5 cm/s), resulting in a capillary Reynolds number of 28.4 and a particle (cell) Peclet number of 0.22. Other experimental conditions employed were an ambient pH (5.5 to 5.7) and a temperature of 25°C ( $\pm 1^\circ$ C). Error bars indicate 1 standard deviation.

solution, which would decrease the diffusive transport of cells towards the substrate surface.

**Bacterial deposition onto alginate conditioning film.** The impact of alginate conditioning films on bacterial adhesion was studied by measuring the efficiencies of attachment of motile and nonmotile bacteria onto either clean or alginate-coated quartz (Fig. 7). The attachment efficiencies of bacteria corresponded to their deposition rates at a given ionic strength as normalized by the deposition rate at the same ionic strength under favorable conditions (Fig. 6). For ionic strengths greater than 100 mM, the deposition rate at 100 mM under favorable conditions was used in the determination of attachment efficiencies. The attachment efficiency reflects the effect of cell-surface interactions on deposition kinetics (46).

For the nonmotile PAO1  $\Delta fliC \Delta pilA$  bacteria, a major enhancement in the efficiency of attachment to an alginate-conditioned substrate compared to that of clean quartz was observed (Fig. 7A). The efficiencies of attachment to the conditioning film were on average three times higher than those to clean quartz, as the efficiencies for the two substrates increased similarly with increasing ionic strength. The maximum attachment efficiencies (set at 1) for the alginate-coated and clean systems were approached at 30 and 300 mM, respectively.

These ionic strengths corresponded to favorable conditions for bacterial deposition in a transport-limited regime. These results suggest that the alginate conditioning film does favorably affect the deposition of nonmotile PAO1 bacteria.

Deposition efficiencies (Fig. 7B) of motile PAO1  $\Delta pilA$  bacteria were less sensitive to the presence of the conditioning film than those of nonmotile bacteria. The efficiencies of deposition onto the conditioned surface at ionic strengths below 100 mM were only about 1.5 times higher than those onto the clean surface. However, as the ionic strength approached 100 mM, the rate of cell transfer onto alginate films rapidly increased (data not shown), similar to the transfer rate measured under favorable conditions (Fig. 6), and the attachment efficiencies neared unity (Fig. 7B). This phenomenon appeared to be very specific to the ionic strength of 100 mM, as suggested by the subsequent reduction in attachment efficiency at 300 mM KCl.

**Role of bacterial motility.** Our results indicate the paramount importance of swimming motility for the deposition of microorganisms onto clean and alginate-conditioned surfaces. Independent of the substrate type, deposition rates measured under favorable (nonrepulsive) conditions confirmed the considerable impact of swimming motility on cell transport towards the substrate. We also demonstrated that under favorable deposition conditions, i.e., deposition onto PLL (Fig. 6) or onto alginate-coated quartz at high ionic strengths (Fig. 7B), an electrolyte concentration of 100 mM KCl optimized the functions of the flagella. An ionic strength of 100 mM approaches the electrolyte condition of physiological saline solutions (0.9% NaCl, or an ionic strength of 154 mM) that is optimal for maintaining the electrolyte balance required by the rotation mechanisms of the flagella (5).

On bare quartz substrate, the physical presence of flagella, in addition to their functions, directly affects bacterial deposition. The general increase in deposition efficiencies of both motile and nonmotile bacteria with increasing ionic strengths suggests that electrostatic interactions are important in deposition. Zeta potential measurements demonstrated that the cells (Fig. 4) and the substrate (Fig. 5) maintain negative charges at their surfaces, which would result in repulsive electrostatic interactions as the separation distance between the cell and the substrate decreases. However, on bare quartz, motile cells have greater attachment efficiencies over the entire range of ionic strengths and approach the maximum attachment efficiency at a lower ionic strength than nonmotile bacteria, despite the similar zeta potentials of the motile and nonmotile strains. Our results support two previously suggested hypotheses involving flagella in bacterial deposition: (i) the kinetic energy of swimming cells enables the cells to overcome the repulsive energy barrier and adhere to regions of heterogeneity on the surface (28), and (ii) the flagella are able to penetrate a repulsive electrostatic barrier and reach areas of heterogeneity at the surface to induce the initial reversible adhesion of the bacteria (30).

On an alginate-coated substrate, the changes in the structure and properties of the conditioning film with increasing electrolyte concentrations can affect bacterial deposition. We observed that the alginate film increased the magnitude of the negative zeta potential of the quartz substrate (Fig. 5) and simultaneously enhanced the attachment efficiencies of nonmotile bacteria compared to those measured for bare quartz

(Fig. 7A). These results suggest that, despite electrostatic repulsion, other interactions, such as biologically specific interactions, may aid in the deposition of microorganisms onto alginate films. However, the deposition efficiencies of motile bacteria in the presence of alginate were only slightly enhanced. Two specific features of the strains may generate other types of interaction with the conditioning film that may explain the observed differences in deposition between the motile and nonmotile strains: (i) the steric impact of the presence of flagella on the cell environment and (ii) the strong hydrophobicity of nonmotile cells. Both factors can influence deposition, depending on the structure of the polyelectrolyte film.

According to our previous studies on the viscoelastic properties of alginate films (14), the structure and properties of the adsorbed layer are highly sensitive to changes in electrolyte concentrations. At low and moderate ionic strengths (about 30 mM), the alginate layer is fluid and exhibits a brush structure due to significant electrostatic repulsion between the extended polyelectrolytes adsorbed onto the substrate. As the ionic strength increases (>30 mM), the layer compacts through alginate coiling and adopts a rigid structure presenting a smoother film-liquid interface. Each structure has specific surface characteristics that can induce attractive and repulsive interactions with the approaching bacterial cells. Hydrophobic interactions between the brush layer and approaching nonmotile cells can develop. The hydrophobic characteristic of the cell surface was previously shown to govern the deposition of *P. aeruginosa* cells onto a poly(ethylene oxide) brush layer (36).

Steric interactions between the alginate brush structure and flagellated bacteria may hinder bacterial deposition. The steric repulsive barrier between extended polymer brushes was shown to maintain large separation distances between particles and the substrate and to prevent the development of attractive interactions (6). Steric interactions between the flagella and the alginate brush may cause the sudden reversal of the swimming direction of the cell, which is a common swimming response of other flagellated bacteria confronting obstacles (9). However, these steric conditions were not permanent in our system. Our results demonstrated that the steric repulsive barrier was suppressed through increases in ionic strength up to 100 mM, which enabled microbial deposition as a result of (i) the optimization of the swimming mobility of the cells, (ii) the compaction of the film by the coiling of the alginate polymers, and (iii) the suppression of electrostatic repulsion due to the decrease in magnitude of the negative zeta potentials of the substrate and cell surfaces.

In conclusion, our research demonstrated that motility plays an important role in the deposition of bacteria onto clean and fouled or conditioned surfaces in aquatic systems. We established a model system that includes (i) well-characterized bacterial strains and (ii) well-defined conditioning of a characteristic substrate with representative polyelectrolytes. The responses of the system to bacterial motility, to changes in ionic strength, and to the presence of an alginate conditioning film were clearly indicative of the impact of these factors on bacterial deposition. The developed alginate conditioning film provided conclusive results that support our approach to understanding the impact of more complex conditioning films on bacterial deposition in natural, engineered, and biomedical aquatic systems.

## ACKNOWLEDGMENTS

This work was supported by the WaterCAMPWS, a Science and Technology Center of Advanced Materials for the Purification of Water with Systems, under National Science Foundation agreement number CTS-0120978.

We thank Barbara Kazmierczak and Maria Lebron for their assistance with the strain constructions and Southern blots and M. Pypaert for his help with the transmission electron microscopy imaging.

## REFERENCES

- An, Y. H., and R. J. Friedman. 1998. Concise review of mechanisms of bacterial adhesion to biomaterial surfaces. *J. Biomed. Mater. Res.* **43**:338–348.
- Aususet, J. B., R. Brent, R. E. Kingston, D. D. Moore, J. G. Seidman, J. A. Smith, and K. Struhl. 1992. Short protocols in molecular biology. Green Publishing and John Wiley & Sons, New York, NY.
- Baker, J. S., and L. Y. Dudley. 1998. Biofouling in membrane systems: a review. *Desalination* **118**:81–89.
- Bakker, D. P., J. W. Klijnstra, H. J. Busscher, and H. C. van der Mei. 2003. The effect of dissolved organic carbon on bacterial adhesion to conditioning films adsorbed on glass from natural seawater collected during different seasons. *Biofouling* **19**:391–397.
- Berg, H. C. 2003. The rotary motor of bacterial flagella. *Annu. Rev. Biochem.* **72**:19–54.
- Biggs, S. 1995. Steric and bridging forces between surfaces fearing adsorbed polymer: an atomic-force microscopy study. *Langmuir* **11**:156–162.
- Busscher, H. J., and A. H. Weerkamp. 1987. Specific and nonspecific interactions in bacterial adhesion to solid substrata. *FEMS Microbiol. Rev.* **46**:165–173.
- Camesano, T. A., and B. E. Logan. 1998. Influence of fluid velocity and cell concentration on the transport of motile and nonmotile bacteria in porous media. *Environ. Sci. Technol.* **32**:1699–1708.
- Cisneros, L., C. Dombrowski, R. E. Goldstein, and J. O. Kessler. 2006. Reversal of bacterial locomotion at an obstacle. *Phys. Rev. E* **73**:030901.
- Costerton, J. W., Z. Lewandowski, D. E. Caldwell, D. R. Korber, and H. M. Lappin-scott. 1995. Microbial biofilms. *Annu. Rev. Microbiol.* **49**:711–745.
- Dabros, T., and T. G. M. van de Ven. 1983. A direct method for studying particle deposition onto solid surfaces. *Colloid Polym. Sci.* **261**:694–707.
- Dasgupta, N., S. K. Arora, and R. Ramphal. 2004. The flagellar system of *Pseudomonas aeruginosa*, p. 675–698. In J.-L. Ramos (ed.), *Pseudomonas*: genomics, life style and molecular architecture. Plenum Publishers, New York, NY.
- de Kerchove, A. J., and M. Elimelech. 2005. Relevance of electrokinetic theory for “soft” particles to bacterial cells: implications for bacterial adhesion. *Langmuir* **21**:6462–6472.
- de Kerchove, A. J., and M. Elimelech. 2006. Structural growth and viscoelastic properties of adsorbed alginate layers in monovalent and divalent salts. *Macromolecules* **39**:6558–6564.
- Elimelech, M. 1994. Effect of particle size on the kinetics of particle deposition under attractive double-layer interactions. *J. Colloid Interface Sci.* **164**:190–199.
- Elimelech, M. 1992. Predicting collision efficiencies of colloidal particles in porous media. *Water Res.* **26**:1–8.
- Elimelech, M., J. Gregory, X. Jia, and R. A. Williams. 1995. Particle deposition and aggregation: measurement, modeling and simulation. Butterworth-Heinemann, Oxford, United Kingdom.
- Gomez-Suarez, C., J. Pasma, A. J. van der Borden, J. Wingender, H. C. Flemming, H. J. Busscher, and H. C. van der Mei. 2002. Influence of extracellular polymeric substances on deposition and redeposition of *Pseudomonas aeruginosa* to surfaces. *Microbiology* **148**:1161–1169.
- Gottenbos, B., H. C. van der Mei, and H. J. Busscher. 2000. Initial adhesion and surface growth of *Staphylococcus epidermidis* and *Pseudomonas aeruginosa* on biomedical polymers. *J. Biomed. Mater. Res.* **50**:208–214.
- Grobe, S., J. Wingender, and H. G. Truper. 1995. Characterization of mucoid *Pseudomonas aeruginosa* strains isolated from technical water systems. *J. Appl. Bacteriol.* **79**:94–102.
- Habash, M. B., H. C. van der Mei, G. Reid, and H. J. Busscher. 1997. Adhesion of *Pseudomonas aeruginosa* to silicone rubber in a parallel plate flow chamber in the absence and presence of nutrient broth. *Microbiology (Reading, United Kingdom)* **143**:2569–2574.
- Hall-Stoodley, L., J. W. Costerton, and P. Stoodley. 2004. Bacterial biofilms: from the natural environment to infectious diseases. *Nat. Rev. Microbiol.* **2**:95–108.
- Kazmierczak, B. I., M. B. Lebron, and T. S. Murray. 2006. Analysis of FimX, a phosphodiesterase that governs twitching motility in *Pseudomonas aeruginosa*. *Mol. Microbiol.* **60**:1026–1043.
- Lee, W., S. Kang, and H. Shin. 2003. Sludge characteristics and their contribution to microfiltration in submerged membrane bioreactors. *J. Memb. Sci.* **216**:217–227.
- Li, Q., and B. E. Logan. 1999. Enhancing bacterial transport for bioaugmentation of aquifers using low ionic strength solutions and surfactants. *Water Res.* **33**:1090–1100.
- Manka, J., and M. Rebhun. 1982. Organic groups and molecular-weight distribution in tertiary effluents and renovated waters. *Water Res.* **16**:399–403.
- Marshall, K. C. 1985. Mechanisms of bacterial adhesion at solid-water interfaces, p. 133–161. In D. C. Savage and M. Fletcher (ed.), *Bacterial adhesion: mechanisms and physiological significance*. Plenum Press, New York, NY.
- Marshall, K. C., R. Stout, and R. Mitchell. 1971. Mechanism of initial events in sorption of marine bacteria to surfaces. *J. Gen. Microbiol.* **68**:337–348.
- Mattick, J. S. 2002. Type IV pili and twitching motility. *Annu. Rev. Microbiol.* **56**:289–314.
- Meadows, P. S. 1971. Attachment of bacteria to solid surfaces. *Arch. Mikrobiol.* **75**:374–381.
- Melo, L. F., and T. R. Bott. 1997. Biofouling in water systems. *Exp. Therm. Fluid Sci.* **14**:375–381.
- Pembrey, R. S., K. C. Marshall, and R. P. Schneider. 1999. Cell surface analysis techniques: what do cell preparation protocols do to cell surface properties? *Appl. Environ. Microbiol.* **65**:2877–2894.
- Pratt, L. A., and R. Kolter. 1998. Genetic analysis of *Escherichia coli* biofilm formation: roles of flagella, motility, chemotaxis and type I pili. *Mol. Microbiol.* **30**:285–293.
- Ramos, H. C., M. Rumbo, and J. C. Sirard. 2004. Bacterial flagellins: mediators of pathogenicity and host immune responses in mucosa. *Trends Microbiol.* **12**:509–517.
- Record, M. T., E. S. Courtenay, D. S. Cayley, and H. J. Guttman. 1998. Responses of *E. coli* to osmotic stress: large changes in amounts of cytoplasmic solutes and water. *Trends Biochem. Sci.* **23**:143–148.
- Roosjen, A., H. J. Busscher, W. Nordel, and H. C. van der Mei. 2006. Bacterial factors influencing adhesion of *Pseudomonas aeruginosa* strains to a poly(ethylene oxide) brush. *Microbiology* **152**:2673–2682.
- Schneider, R. P., B. R. Chadwick, J. Jankowski, and I. Acworth. 1997. Determination of physicochemical parameters of solids covered with conditioning films from groundwaters using contact angles. Comparative analysis of different thermodynamic approaches utilizing a range of diagnostic liquids. *Colloids Surf. A* **126**:1–23.
- Schweizer, H. P., and T. T. Hoang. 1995. An improved system for gene replacement and *xylE* fusion analysis in *Pseudomonas aeruginosa*. *Gene* **158**:15–22.
- Stover, C. K., X. Q. Pham, A. L. Erwin, S. D. Mizoguchi, P. Warrenner, M. J. Hickey, F. S. L. Brinkman, W. O. Hufnagle, D. J. Kowalik, M. Lagrou, R. L. Garber, L. Goltry, E. Tolentino, S. Westbrook-Wadman, Y. Yuan, L. L. Brody, S. N. Coulter, K. R. Folger, A. Kas, K. Larbig, R. Lim, K. Smith, D. Spencer, G. K. S. Wong, Z. Wu, I. T. Paulsen, J. Reizer, M. H. Saier, R. E. W. Hancock, S. Lory, and M. V. Olson. 2000. Complete genome sequence of *Pseudomonas aeruginosa* PAO1, an opportunistic pathogen. *Nature* **406**:959–964.
- Tenke, P., B. Kovacs, M. Jackel, and E. Nagy. 2006. The role of biofilm infection in urology. *World J. Urol.* **24**:13–20.
- Textier, A. C., Y. Andres, M. Illemassene, and P. Le Cloirec. 2000. Characterization of lanthanide ions binding sites in the cell wall of *Pseudomonas aeruginosa*. *Environ. Sci. Technol.* **34**:610–615.
- Tufenkji, N. 5 October 2006, posting date. Application of a dual deposition mode model to evaluate transport of *Escherichia coli* D21 in porous media. *Water Resour. Res.* **42**:W12S11. doi:10.1029/2005WR004851.
- van Hoogmoed, C. G., M. van der Kuijl-Booij, H. C. van der Mei, and H. J. Busscher. 2000. Inhibition of *Streptococcus mutans* NS adhesion to glass with and without a salivary conditioning film by biosurfactant-releasing *Streptococcus mitis* strains. *Appl. Environ. Microbiol.* **66**:659–663.
- Verma, A., M. Schirm, S. K. Arora, P. Thibault, S. M. Logan, and R. Ramphal. 2006. Glycosylation of b-type flagellin of *Pseudomonas aeruginosa*: structural and genetic basis. *J. Bacteriol.* **188**:4395–4403.
- Walker, S. L., J. E. Hill, J. A. Redman, and M. Elimelech. 2005. Influence of growth phase on adhesion kinetics of *Escherichia coli* D21g. *Appl. Environ. Microbiol.* **71**:3093–3099.
- Walker, S. L., J. A. Redman, and M. Elimelech. 2004. Role of cell surface lipopolysaccharides in *Escherichia coli* K12 adhesion and transport. *Langmuir* **20**:7736–7746.
- Yakushi, T., J. H. Yang, H. Fukuoka, M. Homma, and D. F. Blair. 2006. Roles of charged residues of rotor and stator in flagellar rotation: comparative study using H<sup>+</sup>-driven and Na<sup>+</sup>-driven motors in *Escherichia coli*. *J. Bacteriol.* **188**:1466–1472.